SLAC–PUB–7855
June 1998

First Bunch Length Studies in the SLC South Final Focus*

F. Zimmermann, G. Yocky, D.H. Whittum, K.A. Thompson, C. Ng,
D. McCormick, T. Markiewicz, and K.L.F. Bane

Stanford Linear Accelerator Center
Stanford University, Stanford, CA 94309, USA

We report the first studies of bunch length in collision in an operating linear collider, making use of a new rf bunch length monitor installed in the South Final Focus of the Stanford Linear Collider (SLC) prior to the 1997/98 luminosity run. The theoretical and measured monitor responses to linac injection phase and bunch compressor voltage are described. Correlations with beamstrahlung and luminosity are discussed.

Presented at the
6th European Particle Accelerator Conference (EPAC-98)
Stockholm, Sweden, June 22–26, 1998

*Work supported by the U.S. Department of Energy contract DE–AC03–76SF00515.

FIRST BUNCH LENGTH STUDIES IN THE SLC SOUTH FINAL FOCUS*

F. Zimmermann, G. Yocky, D.H. Whittum, K.A. Thompson, C. Ng, D. McCormick, T. Markiewicz, and K.L.F. Bane, SLAC, Stanford University, Stanford, USA

Abstract

We report the first studies of bunch length in collision in an operating linear collider, making use of a new rf bunch length monitor installed in the South Final Focus of the Stanford Linear Collider (SLC) prior to the 1997/98 luminosity run. The theoretical and measured monitor responses to linac injection phase and bunch compressor voltage are described. Correlations with beamstrahlung and luminosity are discussed.

1 INTRODUCTION

In 1997, a multi-channel rf bunch-length monitor (BLM) was installed in the SLC South Final Focus [1], in order to permit control of the interaction-point (IP) bunch length of both colliding beams. The bunch length at the SLC IP is affected by many variables, most notably the injection time into the linac, the voltage of the bunch compressor rf, the R_{56} value of the ring-to-linac transport line (RTL), the beam distribution and the bunch charge. The bunch length is expected to affect the SLC luminosity, because of hourglass effect (depth of focus) and disruption (mutual contraction of the two beams during the collision). Bunch-length control was of particular interest in the 1997/98 SLC run, where the luminosity enhancement factor H_D [5], due to disruption, approached 100%.

The BLM consists of a ceramic gap in the beam pipe, a 50-m long X-band waveguide, and a multi-channel signal processing unit [1]. When a beam passes this gap, electromagnetic radiation is emitted, whose frequency spectrum contains information about the bunch length. During BLM commissioning it was found that monitor channel 3, detecting the rf power radiated above 21 GHz, provides the most useful signal, and all measurements reported here refer to this channel.

The BLM signal is proportional to the square of the bunch charge and it decreases with increasing bunch length. To remove the dependence on the bunch charge, we normalize the signal by subtracting the pedestal and dividing by the number of particles in units of 10^{10}. For example, at the nominal bunch population of $N_b = 4\times10^{10}$, a normalized signal of 10 corresponds to about 160 counts of the gated ADC, and the resolution limit due to digitization is about 0.6%.

2 SENSITIVITY

In the SLC, one major source of IP bunch-length variation are changes in the linac injection phase, which are caused by thermal rf phase drifts. Such linac phase errors introduce a position-energy correlation along the bunch. The correlated energy spread then changes the IP bunch length via momentum compaction (R_{56}) in the 1.2-km long collider arcs.

In Fig. 1 we depict the measured and simulated BLM signal as a function of the linac injection phase. The figure demonstrates that the BLM can resolve pulse-to-pulse changes in the linac injection phase of less than one degree S-band (2.8 GHz). In the simulation, 10^4 particles were tracked in longitudinal phase space from the damping ring to the IP, and the beam power spectrum above 21 GHz was obtained by applying an FFT to the final distribution. Over the scan range considered, the simulated IP bunch length varies by more than a factor of 3, with an associated dramatic change in the shape of the beam distribution. The source of the overall additive offset on the left axis is unclear. Instrumental effects being ruled out, it could indicate high-frequency fine structure in the beam.

Figure 2 illustrates the response of the BLM signal to changes in the compressor voltage. The total scan range corresponds to an expected change in the rms bunch length by a factor of 1.7 (from 1.1 mm to 1.8 mm).

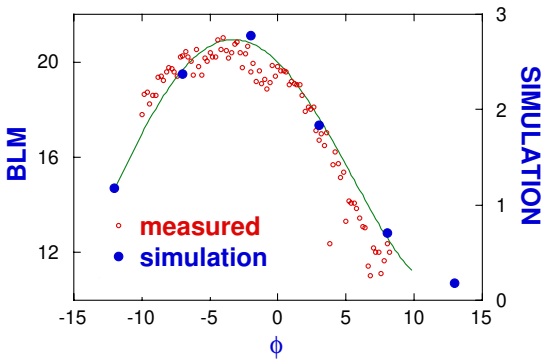

Figure 1: BLM signal vs. linac injection time in degree S-band, for $N_b \approx 1.2\times10^{10}$ with energy and RTL feedbacks active; each data point corresponds to one beam pulse; a simulation result (arbitrary units) is also shown.

The BLM signal was calibrated by recording, over a few hundred pulses, both BLM signal and beam intensities for several different combinations of linac injection phase and compressor voltage. For each parameter setting, the beam energy profile at the end of the linac was also measured, using a wire scanner at a dispersive location.

Again, the corresponding IP distributions and bunch lengths were obtained from a multi-particle tracking simulation of the longitudinal beam transport. In the tracking, compressor voltage, compressor phase and the abso-

* Work supported by the U.S. Department of Energy under contract DE-AC03-76SF00515.

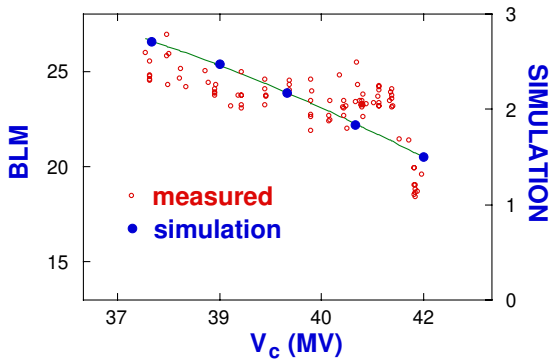

Figure 2: BLM signal vs. compressor voltage in MV, for $N_b \approx 1.5 \times 10^{10}$; each data point corresponds to one beam pulse. A simulation result (arbitrary units) is shown for comparison.

lute offset of the linac phase were adjusted by fitting, so as to optimize the agreement between the simulated and measured energy profiles at the end of the linac [2]. The bunch compression, or anti-compression, in the arc was then calculated in a second simulation step, starting with the fitted end-of-linac distribution. The simulated bunch-length evolution was confirmed independently, by measuring the variation of the wakefield-induced energy loss per unit length along the arc [3], utilizing the fact that the wakefield depends on the bunch length.

Figure 3 shows the normalized BLM signal versus the simulated rms IP bunch length. The figure indicates that IP beam distributions with the same rms bunch length give rise to very similar BLM signals. We attribute scatter in the data points to differences in the shape of the distributions for different compressor voltages, amounting to a 10% variation in rms bunch length.

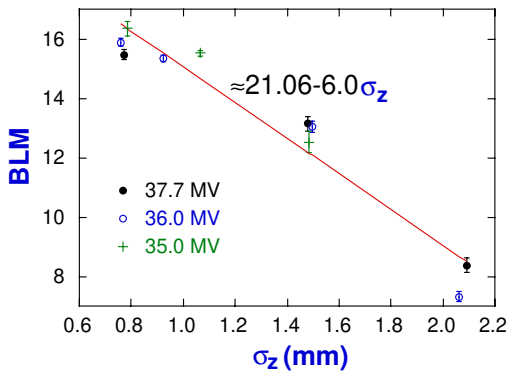

Figure 3: Calibration: measured BLM signal vs. rms IP bunch length determined from a fit to the linac energy profile and subsequent simulation of the beam transport through the SLC South arc; for each value of the compressor voltage the IP bunch length was varied by changing the injection time into the linac; each data point derives from an average over 100 beam pulses, with rms variation shown by the error bars.

3 BEAM-BEAM STUDIES

Both the luminosity and the beamstrahlung (synchrotron radiation in the field of the opposing beam) depend on the bunch length. For a Gaussian bunch profile with rms length σ_z and centered collisions (indicated by a subindex '0'), the total energy loss of the electron beam due to beamstrahlung in the field of the positron beam is [5]:

$$\Delta E_0^{e^-} \approx 0.22 \, \frac{r_e^3 N_{e^-} N_{e^+}^2 \gamma}{\sigma_{z,e^+}} \left(\frac{2}{\sigma_x + \sigma_y} \right)^2 \qquad (1)$$

where $r_e \approx 2.8 \times 10^{-15}$ m is the classical electron radius, and σ_x and σ_y are the transverse IP beam sizes, which here are taken to be the same for both beams. The energy loss per electron, $\Delta E_0^{e^-}/N_{e^-}$, is proportional to $N_{e^+}^2/\sigma_{z,e^+}$, roughly the same dependence as expected for the BLM raw signal (*i.e.*, not normalized to the current). Similarily, the specific luminosity $L_0/(N_{e^-} N_{e^+})$ is a function of the bunch length, due to hourglass effect and disruption.

We have simulated the dependence of beamstrahlung and luminosity on the bunch length using the code Guinea-Pig [4], for typical 1997 SLC parameters: bunch population $N_b \approx 3.5 \times 10^{10}$, rms beam sizes $\sigma_{x,y} \approx 1.70, 0.92$ μm, rms divergences $\theta_{x,y} \approx 460, 260$ μrad, and considering realistic (non-Gaussian) longitudinal distributions. The results are summarized in Figs. 4 and 5.

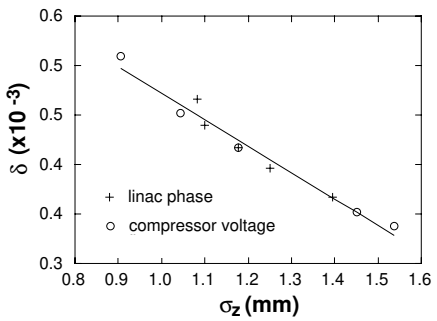

Figure 4: Simulated average energy loss due to beamstrahlung as a function of rms IP bunch length, varied via compressor voltage and linac phase.

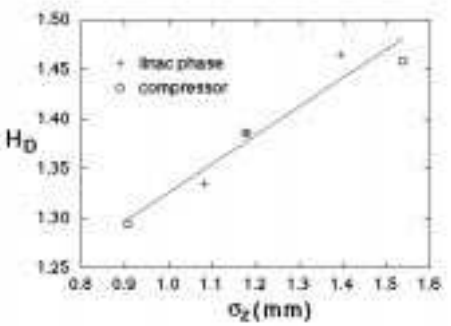

Figure 5: Simulated luminosity enhancement factor H_D as a function of rms IP bunch length, varied via compressor voltage and linac phase.

The measurements described in the following explore the correlations between the BLM signal and luminosity or beamstrahlung. Unlike the scans shown earlier, the data for these studies were collected in a *parasitic* mode, taking advantage of the natural pulse-to-pulse bunch-length variation. This natural variation is only a few percent, and its effect is easily shadowed by fluctuations in other variables.

We can express the rms variation of the electron-beam energy loss due to beamstrahlung as

$$\frac{\Delta E^{e^-}_{\rm rms}}{\Delta E^{e^-}_{\rm av}} \approx \sqrt{2}\left(\frac{y_{\rm rms}}{\sigma_y}\right)^2 + \sqrt{2}\left(\frac{x_{\rm rms}}{\sigma_x}\right)^2 + \frac{\sigma_{z\ {\rm rms}}}{\sigma_{z\ {\rm av}}} + 2\,\frac{(\sigma_x+\sigma_y)_{\rm rms}}{(\sigma_x+\sigma_y)_{\rm av}} + 2\,\frac{N_{e^+,{\rm rms}}}{N_{e^+,{\rm av}}} + \frac{N_{e^-,{\rm rms}}}{N_{e^-,{\rm av}}} \quad (2)$$

where $x_{\rm rms}$, $y_{\rm rms}$ denote the rms beam-beam separation in the horizontal and vertical plane. For simplicity, in Eq. (2) we have assumed that the sizes of both beams are the same and fluctuate synchronously. For the luminosity we have

$$\frac{L_{\rm rms}}{L_{\rm av}} \approx \frac{\sqrt{2}}{4}\left(\frac{y_{\rm rms}}{\sigma_y}\right)^2 + \frac{\sqrt{2}}{4}\left(\frac{x_{\rm rms}}{\sigma_x}\right)^2 + \frac{1}{4}\,\frac{\sigma_{z,{\rm rms}}}{\sigma_{z,{\rm av}}} + \frac{\sigma_{x,{\rm rms}}}{\sigma_{x,{\rm av}}} + \frac{\sigma_{y,{\rm rms}}}{\sigma_{y,{\rm av}}} + \frac{N_{e^+,{\rm rms}}}{N_{e^+,{\rm av}}} + \frac{N_{e^-,{\rm rms}}}{N_{e^-,{\rm av}}} \quad (3)$$

where the coefficient $1/4$ in front of the bunch length term approximates the simulation result of Fig. 5. From Eq. (2) and (3), and noting that $(x,y)_{\rm rms}/\sigma_{x,y} \approx 30$–$50\%$, $(\sigma_x+\sigma_y)_{\rm rms}/(\sigma_x+\sigma_y)_{\rm av} \approx 20$–$30\%$, $N^{e^+,e^-}_{\rm rms}/N^{e^+,e^-}_{\rm av} \approx 1$–$3\%$, and $\sigma_{z,{\rm rms}}/\sigma_{z,{\rm av}} \approx 5\%$ (a result of the BLM measurements), the effect of pulse-to-pulse bunch-length fluctuation on beamstrahlung and luminosity is found to be small compared with the variation induced by other sources, such as changes in the beam-beam separation.

Fluctuations in bunch population are corrected for with toroid readings. We also attempt to remove the dependence on the beam-beam separation $(x,y)_{\rm rms}$, by fitting the data to a 2nd order Taylor expansion of the beamstrahlung signal as a function of the horizontal and vertical deflection angles $\theta_{x,y}$, since for small offsets the deflection is proportional to the beam-beam separation. The deflection angles are inferred from orbit readings at 2 BPMs on either side of the IP. In the same way, we expand the energy loss ΔE to second order in θ_x and θ_y, with coefficients obtained by fitting. We then can, for every beam pulse, calculate position-corrected values L_0 and ΔE_0, accurate for small beam-beam separations.

A signal proportional to the beamstrahlung induced energy loss $\Delta E^{e^-}_0$ is obtained from a monitor detecting photons radiated by the electron beam at the collision point [6]. Figure 6 (top) shows, for 100 beam pulses, the correlation of this beamstrahlung signal with the squared intensity of the positron beam, $N^2_{e^+}$, and with the raw (not normalized) BLM signal. The latter shows a better correlation, which is expected because it contains additional (bunch length) information. Figure 6 (bottom) reveals little correlation between the specific luminosity (a signal from a radiative Bhabha monitor, divided by the two bunch charges) and the normalized BLM signal.

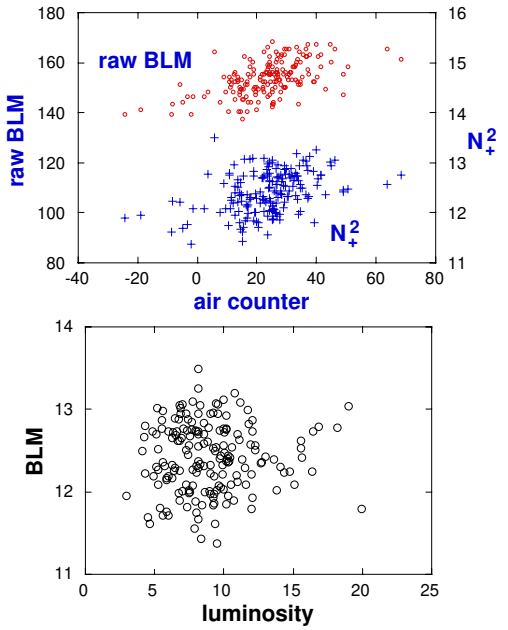

Figure 6: Positron intensity squared, $N^2_{e^+}$ (10^{20}), and raw BLM signal vs. e^- beamstrahlung signal (top); normalized BLM signal vs. specific luminosity signal (bottom).

4 CONCLUSIONS

The rf BLM in the SLC South Final Focus can monitor pulse-to-pulse changes in the IP bunch length of both colliding beams, with a precision of a few percent. Its response to linac injection time and compressor voltage is consistent with simulations of the longitudinal beam transport. Pulse-to-pulse fluctuation in beamstrahlung and luminosity is caused primarily by variation in the beam-beam separation and, possibly, in the beam sizes. The bunch length is not a dominant source of short-term fluctuation.

5 REFERENCES

[1] F. Zimmermann, *et al.*, "An RF Bunch-Length Monitor for the SLC Final Focus", Proc. of IEEE PAC 97, Vancouver, SLAC-PUB-7456 (1997).

[2] K.L.F. Bane, *et al.*, "Measurement of the Longitudinal Wakefield and the Bunch Shape in the SLAC Linac", Proc. of IEEE PAC 97, Vancouver, SLAC-PUB-7536 (1997).

[3] K.L.F. Bane, *et al.*, "Measurements of Longitudinal Wakefields in the SLC Collider Arcs", Proc. of First APAC, Tsukuba, SLAC-PUB-7781 (1998).

[4] D. Schulte, "Study of Electromagnetic and Hadronic Background in the Interaction Region of the TESLA Collider", Ph.D. thesis, University of Hamburg (1996).

[5] K. Yokoya and P. Chen, "Beam-beam phenomena in linear colliders", Lecture at 1990 US-CERN School on Particle Accelerators, Hilton Head Isl. (1990).

[6] R.C. Field, "Beamstrahlung Monitors at SLC", Nucl. Instrum. Meth. A265, p. 167, SLAC-PUB-4252 (1988).